PERGAMON

International Journal of Solids and Structures 40 (2003) 4637–4657

INTERNATIONAL JOURNAL OF SOLIDS and STRUCTURES

www.elsevier.com/locate/ijsolstr

Deployment of tensegrity structures

Cornel Sultan [a,*], Robert Skelton [b]

[a] *Medical School, Harvard University, Boston, MA 02115, USA*
[b] *University of California, La Jolla, CA 92093-0411, USA*

Received 30 April 2003

Abstract

In this paper we present a strategy for tensegrity structures deployment. The main idea is to use a certain set of equilibria to which the undeployed and deployed configurations belong. In the state space this set is represented by an equilibrium manifold. The deployment is conducted such that the deployment trajectory is close to this equilibrium manifold.

Keywords: Structures; Tensile; Equilibrium

1. Introduction

Deployable structures are widely used for solar arrays, antennas, spacecraft as well as for retractable roofs and shelters. Until recently these applications have been developed mostly by trial and error but the current growing demand for deployable structures requires a more systematic approach aimed at developing new, generic solutions. As it is well known, serious problems in space activity may occur during the deployment of the structures used. Classical deployable structures suffer from several deficiencies, such as the existence of complicated rigid to rigid joints and the use of telescopic struts for deployment. One promising solution to eliminate these problems is the use of *tensegrity structures* as deployable structures.

Tensegrity structures represent a class of space structures composed of a set of *soft* members and a set of *hard* members. The soft members cannot carry other significant loads except for tensile ones. The representative example is an elastic tendon which cannot be compressed for all practical purposes but can carry significant tension. Because of this property we shall also refer to these members as *tensile* members. On the other hand the hard members are characterized by the fact that they can carry any type of load. The representative example is a bar which can carry significant and comparable tension, compression forces, bending moments, etc.

* Corresponding author. Tel.: +1-617-381-0013; fax: +1-617-234-9876.
E-mail addresses: cornel.sultan@tch.harvard.edu (C. Sultan), bobskelton@ucsd.edu (R. Skelton).

0020-7683/03/$ - see front matter © 2003 Elsevier Ltd. All rights reserved.
doi:10.1016/S0020-7683(03)00267-1

Nomenclature

b	length of the base and top triangles sides
$\hat{b}_{1,2,3}$	inertial reference frame unit vectors
d	coefficient of friction at all joints
h	overlap
k_*	stiffness of tendon * (* can be j, S, V, D)
l	length of a bar
l_j	length of the jth tendon
l_0	vector of tendons rest-lengths
l_{0_j}	rest-length of tendon j
m	mass of a bar
q	vector of independent generalized coordinates
q_e	vector of independent generalized coordinates in a symmetrical prestressable configuration
s	degree of polynomials
x	state vector
$x_d(t)$	deployment path
$x_e(t)$	equilibrium path
t	time
$\hat{t}_{1,2,3}$	top reference frame unit vectors
$A(q)$	equilibrium matrix
$C(q)$	damping matrix
D	length of a diagonal tendon in a symmetrical configuration
D_0	rest-length of a diagonal tendon for the SVD tensegrity structure
E_b	Young's modulus of a bar
E_*	Young's modulus of tendon *
F	vector of external forces and torques
$H(q)$	disturbance matrix
J	transversal moment of inertia of a bar
$J_{1,2,3}$	moments of inertia of the rigid top
$M(q)$	inertia matrix
M_i	friction torque at joint i
M_t	mass of the top
N_t	number of tendons
R	exterior radius of a bar
P	pretension coefficient
S	length of a saddle tendon in a symmetrical configuration
S_0	rest-length of a saddle tendon for the SVD tensegrity structure
V_0	rest-length of a vertical tendon for the SVD tensegrity structure
X, Y, Z	Cartesian inertial coordinates of the mass center of the top
$T(q)$	vector of tensions in the tendons
T_j	tension in the jth tendon
$U_{d/u}$	potential energy at the deployed/undeployed configuration
V	length of a vertical tendon in a symmetrical configuration
α	azimuth of bar $A_{11}B_{11}$ in a symmetrical configuration
α_u	undeployed configuration azimuth

α_d	deployed configuration azimuth
α_{ij}	azimuth of bar $A_{ij}B_{ij}$
$\gamma_{b,t}$	safety coefficients
δ	declination of a bar in a symmetrical configuration
δ_u	undeployed configuration declination
δ_d	deployed configuration declination
δ_{ij}	declination of bar $A_{ij}B_{ij}$
$\epsilon_{q,\dot{q}}$	tolerances
ρ	density of a bar
ψ, ϕ, θ	Euler angles of the top reference frame
$\sigma_{*_{max}}$	maximum stress allowed in tendon *
τ	normalized time
ω_i^r	relative angular velocity vector at joint i
T_d	deployment time

A structure composed of soft and hard elements as described above is a tensegrity structure if it has the property of *prestressability*. This property consists of the structure's ability to maintain an equilibrium shape with all tensile members in tension and in the absence of external forces or torques. Tensegrity structures integrity is guaranteed by the tensile members in tension, hence their denomination, *tensegrity*, an acronym of *tension-integrity* coined by Fuller. A perspective view of a tensegrity tower, composed of 33 elastic tendons (soft members), 9 rigid bars, a rigid base, and a rigid top (hard members) is given in Fig. 1.

It is apparent that these structures are capable of large displacement and can easily change their shape. They can also be built without, or with very few, complicated bar to bar joints. They offer excellent opportunities for physically integrated structure and controller design, since the elastic components can carry both the sensing and actuating functions. These structures are very promising deployable structures due to packaging efficiency and ease of deployment, unlike systems with telescopic struts and complicated joints (see Furuya, 1992). Their deployment can be accomplished by controlling the tendons, without involving complicated telescopic struts.

Although the origins of tensegrity structures can be pin-pointed to 1921 (see Motro, 1996), the main investigations have been carried out rather recently. Detailed geometrical studies were first reported by Fuller (1975) and Pugh (1976). Approaches using mechanics were later developed being aimed at establishing the theoretical framework for the analysis and design of these structures. Calladine (1978), Motro et al. (1986), Pellegrino and Calladine (1986), Sultan et al. (2001), made important contributions to the general theory of these structures statics. Sultan et al. (2001), Murakami and Nishimura (2001a,b) and Nishimura and Murakami (2001) published a series of results regarding analytical solutions of the statics problem, while Hanaor (1988), Kebiche et al. (1999), Vassart and Motro (1999), developed numerical methods of large generality. The field of tensegrity structures dynamics research was pioneered by Motro et al. (1986). Significant theoretical advances have been later made by Murakami (2001) and Sultan et al. (2002a,b) who developed nonlinear and linearized dynamics models for tensegrity structures. Using simpler models, Connelly and Whiteley (1996) proved some important results regarding the stability and rigidity of equilibrium configurations, while Oppenheim and Williams (2001a,b) discovered interesting properties of their vibration and damping characteristics. Control design studies have been pioneered by Skelton and Sultan (1997), followed by important contributions by Sultan and Skelton (1997), Djouadi et al. (1998), and Kanchanasaratool and Williamson (2002). Applications of tensegrity structures have been proposed,

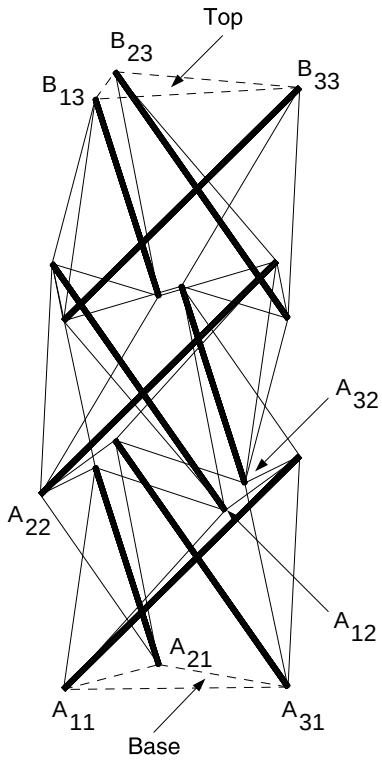

Fig. 1. Three stage tensegrity tower.

ranging from tensegrity domes (Hanaor, 1992; Wang and Liu, 1996), antennas (Djouadi et al., 1998), to tensegrity sensors (Sultan and Skelton, 1998a), space telescopes (Sultan et al., 1999), flight simulators (Sultan et al., 2000).

Of crucial importance for future applications of tensegrity structures is the development of strategies for their deployment. Furuya (1992) examined these structures deployment, but only at the conceptual level. Sultan and Skelton (1998b) analyzed the deployment of tensegrity structures using tendon control and proposed a procedure which will be expanded upon in this article. In another article Sultan et al. (2002a) proposed tendon controlled reconfiguration procedures aimed at changing the equilibrium configuration of a tensegrity structure while preserving its height. Tibert and Pellegrino (2002) developed a procedure which uses telescopic struts for deployment of a tensegrity antenna.

The deployment strategy presented in this paper is a generic solution, based on the existence of a set of equilibrium configurations to which the undeployed and deployed configurations belong. In the state space this set is represented by an equilibrium manifold. The deployment process is conducted such that its state space trajectory is close to the equilibrium manifold. Additional optimization constraints (such as minimum deployment time or minimum energy) can be imposed and the necessary control law solved for. Technologically, the deployment process can be conducted using either tendon control or telescopic struts.

The paper is organized as follows. First, the deployment strategy is presented. Then, for a particular class of tensegrity structures, some results regarding their dynamics and statics are reviewed. Next, the first example of the application of the deployment strategy is given: the time optimal deployment problem is

formulated and numerically solved for a certain tensegrity structure. Finally, the second example is given, presenting the deployment of a more complex tensegrity structure using smooth controls.

2. Deployment strategy

We assume that the structure yields an *initial equilibrium* configuration with all tendons in tension. We want to change this configuration into another *final equilibrium* one, such that certain constraints are met (e.g. the tendons are always in tension throughout the motion, the rigid bodies do not collide, etc.). The process through which the structure changes from one *equilibrium* configuration into another is referred to as *deployment*.

In the following we present a deployment strategy based on the assumption that an *equilibrium manifold* to which the undeployed and deployed configurations belong has been identified. The main idea is to conduct the deployment such that the *deployment path is close enough to this manifold*. The advantage in doing so is that, due to the proximity of the deployment path to this manifold, the successive configurations the structure passes through are not much different from the equilibrium ones. If these equilibrium configurations have certain properties (for example, all tendons are in tension and sufficient clearance between the isolated rigid bodies exists), then the deployment can be conducted *slow enough* such that the intermediate configurations the structure passes through have the same properties.

One way to ensure that the deployment path is close to the equilibrium manifold is by letting the control variables take values only in the set of the equilibrium manifold controls. That is to say the controls are allowed to take only values which correspond to equilibria which belong to the equilibrium manifold. If the change in control variables is smooth enough, then the system undergoes slow motions, remaining close to this manifold. This procedure presents an important, practical, advantage: if the manifold consists only of asymptotically stable equilibria the procedure is fault tolerant in the following sense. If for certain reasons (e.g. power failure) the controls are frozen to some intermediate values, the structure will oscillate and settle down to an equilibrium configuration which belongs to the equilibrium manifold and from which the deployment process can be later restarted.

The control variables can be, for example, the length of the struts (in the case of telescopic struts control), the rest-lengths of the tendons (in the case of tendon control) or a combination of both.

An important step in this deployment strategy is the discovery of the equilibrium manifold. For this purpose a procedure which combines both numerical and symbolic computation, has been proposed and successfully applied to several tensegrity structures by Sultan (1999).

3. Tensegrity structures dynamics

In the following we summarize some results on the dynamics of a certain class of tensegrity structures.

Consider a tensegrity structure composed of *elastic* and *massless* tendons and *rigid* bodies. For mathematical modeling it is assumed that all constraints on the system are *holonomic*, *scleronomic* and *bilateral*, the external constraint forces are *workless*, the forces exerted by other force fields are neglected, external forces and torques are applied only to the rigid elements of the structure, the structure is affected at most by *linear kinetic friction* at the rigid to rigid joints and *linear kinetic damping* in the tendons (linear kinetic friction means that the friction torques/forces are proportional to the relative angular/linear velocities between the members in contact, and linear kinetic damping means that the damping force introduced by a tendon is proportional to the time derivative of its elongation). The equations of motion are (see Sultan et al., 2002a):

$$M(q)\ddot{\boldsymbol{q}} + c(q,\dot{\boldsymbol{q}}) + A(q)T(q) + C(q)\dot{\boldsymbol{q}} + H(q)F = 0, \tag{1}$$

where

- $q = [q_1\ q_2 \cdots q_N]^{\mathrm{T}}$ is the vector of independent generalized coordinates used to describe the structure's configuration, and N is the number of degrees of freedom.
- $M(q)$ is the inertia matrix.
- $c(q, \dot{q})$ is a vector of quadratic functions in $\dot{q}$, whose components can be expressed as:

$$c_i = \sum_{j=1}^{N} \sum_{n=1}^{N} \left(\frac{\partial M_{ij}}{\partial q_n} - \frac{1}{2} \frac{\partial M_{jn}}{\partial q_i} \right) \dot{q}_j \dot{q}_n, \quad i = 1, \ldots, N. \tag{2}$$

- $A(q)T(q)$ is the vector of elastic generalized forces where $A[n, j] = \partial l_j / \partial q_n$, $n = 1, \ldots, N$, $j = 1, \ldots, N_{\mathrm{t}}$, N_{t} being the number of tendons, l_j the length of tendon j, and $T(q)$ the vector of tendons tensions.
- $C(q)\dot{q}$ is a vector of generalized damping forces where $C(q)$ is the damping matrix (this form of generalized damping forces is valid only for the kinetic damping assumption).
- $H(q)F$ is a vector of generalized forces due to external forces and torques where F is the vector of external forces and torques applied to the rigid bodies and $H(q)$ is the disturbance matrix.

These equations have been used to develop *reconfiguration procedures* (Sultan et al., 2002a) and to derive the *linearized* equations of motion of tensegrity structures (Sultan et al., 2002b).

The second order ordinary differential equations of motion, Eq. (1), can be cast in first order form if we introduce the state vector $x = [q^{\mathrm{T}}\ \dot{q}^{\mathrm{T}}]^{\mathrm{T}}$:

$$\dot{x} = f(x), \tag{3}$$

where $f(x)$ is given by

$$f(x) = [\dot{q}^{\mathrm{T}}\ (-M^{-1}(q)(c(q, \dot{q}) + A(q)T(q) + C(q)\dot{q} + H(q)F))^{\mathrm{T}}]^{\mathrm{T}}. \tag{4}$$

This first order form will be later used in this article.

4. Tensegrity structures statics

Because the deployment process consists of transforming one equilibrium configuration of the structure into another, in the following we shall summarize some results on tensegrity structures statics from Sultan et al. (2001).

Equilibrium configurations are mathematically characterized by the condition that in the equations of motion, Eq. (1), all time derivatives are zero. In order to avoid entanglement we also require that the tendons are in tension:

$$A(q)T(q) + H(q)F = 0, \quad T_j > 0, \ \ j = 1, \ldots, N_{\mathrm{t}}, \tag{5}$$

where T_j is the tension in tendon j. Of special interest are particular equilibria defined by the additional condition that no external forces or torques act on the structure ($F = 0$). These equilibria are called *prestressable configurations* and are mathematically characterized by the prestressability conditions:

$$A(q)T(q) = 0, \quad T_j > 0, \ \ j = 1, \ldots, N_{\mathrm{t}}. \tag{6}$$

Sultan (1999) developed a methodology to investigate the prestressability conditions (6). The methodology is aimed at discovering a set of prestressable configurations which can (eventually) be represented by an equilibrium manifold in the state space. The methodology can also be used for equilibrium configurations which occur under nonzero external forces or torques ($F \neq 0$). Sultan et al. (2001) analyzed various tensegrity structures for prestressability using this methodology and discovered equilibrium manifolds. Some of these manifolds will be used in this article for our deployment strategy.

5. Deployment of a two stage SVD tensegrity structure

In the following we give an example of the application of the above strategy to the time optimal deployment of a two stage SVD tensegrity structure. This type of structure has been extensively studied by Sultan et al. (2001, 2002a,b). A prestressable equilibrium manifold to which collapsed configurations (of almost zero height) and erected ones of various heights belong has been discovered (see Sultan et al., 2001). This manifold will be used in our deployment strategy.

5.1. Structure's description

A perspective view of a two stage SVD tensegrity structure is given in Fig. 2. Its components are: a triangular base ($A_{11}A_{21}A_{31}$), a triangular top ($B_{12}B_{22}B_{32}$), 3 bars attached through ball and socket joints to the base ($A_{i1}B_{i1}$), 3 bars similarly attached to the rigid top ($A_{i2}B_{i2}$), and 18 tendons which connect the end points of the bars. Stage j is composed of bars $A_{ij}B_{ij}$, $i = 1, 2, 3$. The tendons are classified as saddle tendons ($B_{i1}A_{j2}$), vertical tendons ($A_{j1}B_{i1}$ and $A_{j2}B_{i2}$), and diagonal tendons ($A_{j1}A_{i2}$ and $B_{j1}B_{i2}$). The assumptions made for mathematical modeling are: the tendons are massless, not damped (i.e. not affected by damping), and linear elastic, the base and the top are rigid bodies, the bars are rigid, axially symmetric, for each bar the rotational degree of freedom around its longitudinal axis of symmetry is neglected, the external force fields (e.g. gravity) are neglected, friction torques which are proportional to the relative angular velocity between the bars and the base or top act at the joints between the top or base with the bars ($M_i = d\omega_i^r$ where M_i, ω_i^r are the friction torque and relative angular velocity at joint i, respectively, and $d < 0$ is the friction coefficient). Hence Eq. (1) applies.

The inertial reference frame, $\hat{b}_1$, $\hat{b}_2$, $\hat{b}_3$, is a dextral set of unit vectors, whose center coincides with the geometric center of the triangle $A_{11}A_{21}A_{31}$. Axis $\hat{b}_3$ is orthogonal to the plane $A_{11}A_{21}A_{31}$ pointing upward,

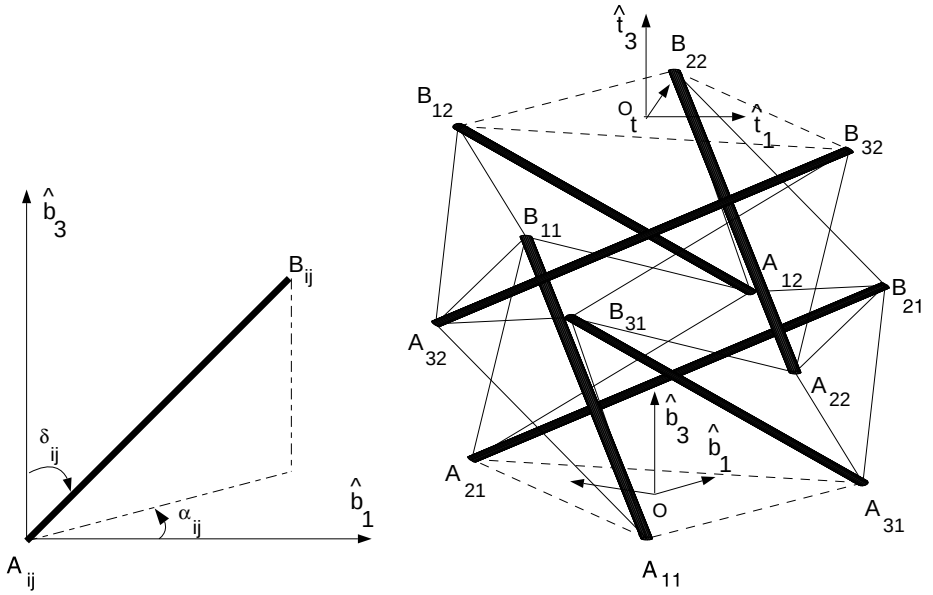

Fig. 2. Two stage SVD tensegrity structure.

while $\hat{b}_1$ is parallel to $A_{11}A_{31}$. The dextral reference frame attached to the rigid top is $\hat{t}_1$, $\hat{t}_2$, $\hat{t}_3$. Its center coincides with the geometric center of the triangle $B_{12}B_{22}B_{32}$ while $\hat{t}_3$ is orthogonal to the plane $B_{12}B_{22}B_{32}$ pointing upward and $\hat{t}_1$ is parallel to $B_{12}B_{32}$. For simplicity it is assumed that this system is central principal for the rigid top (i.e. its center coincides with the center of mass and its axes coincide with the principal axes of the rigid top).

The 18 independent generalized coordinates used to describe this system's configuration are: ψ, ϕ, θ, the Euler angles for a 3-1-2 sequence to characterize top's reference frame orientation in the inertial frame, X, Y, Z, the Cartesian inertial coordinates of the mass center of the top, δ_{ij}, α_{ij}, the declination and the azimuth of bar $A_{ij}B_{ij}$, measured with respect to the inertial reference frame (Fig. 2). Hence the vector of independent generalized coordinates is:

$$q = [\,\delta_{11} \quad \alpha_{11} \quad \delta_{21} \quad \alpha_{21} \quad \delta_{31} \quad \alpha_{31} \quad \delta_{12} \quad \alpha_{12} \quad \delta_{22} \quad \alpha_{22} \quad \delta_{32} \quad \alpha_{32} \quad \psi \quad \phi \quad \theta \quad X \quad Y \quad Z\,]^{\mathrm{T}}. \tag{7}$$

5.2. Equilibrium manifold

Consider a two stage SVD tensegrity structure with the following particularities: all bars are identical (of length l and mass m) and the top and base triangles are equal, equilateral triangles of side b. For simplicity we also assume that all saddle tendons are identical (of rest-length S_0 and stiffness k_{S}), all vertical tendons are identical (of rest-length V_0 and stiffness k_{V}), all diagonal tendons are identical (of rest-length D_0 and stiffness k_{D}). Here the stiffness is defined as the product between the cross-sectional area and the longitudinal elasticity modulus of a tendon.

In Sultan et al. (2001) a particular set of configurations, called *symmetrical configurations*, was defined as follows: all bars have the same declination, δ, the vertical projections of A_{i2}, B_{i1}, $i = 1, 2, 3$ onto the base make a regular hexagon, planes $A_{11}A_{21}A_{31}$ and $A_{12}A_{22}A_{32}$ are parallel. Three quantities are used to parameterize these configurations: α, the azimuth of $A_{11}B_{11}$, δ, and h, the overlap, defined as the distance between planes $B_{11}B_{21}B_{31}$ and $A_{12}A_{22}A_{32}$ and considered positive if $A_{12}A_{22}A_{32}$ is closer to $A_{11}A_{21}A_{31}$ than $B_{11}B_{21}B_{31}$.

At such a configuration the lengths of the saddle, vertical, and diagonal tendons are given by

$$S = \sqrt{h^2 + \frac{b^2}{3} + l^2\sin^2(\delta) - \frac{2}{\sqrt{3}}lb\sin(\delta)\cos\left(\alpha - \frac{\pi}{6}\right)}, \tag{8}$$

$$V = \sqrt{l^2 + b^2 - 2lb\sin(\delta)\sin\left(\alpha + \frac{\pi}{6}\right)}, \tag{9}$$

$$D = \sqrt{l^2 + \frac{b^2}{3} + h^2 - 2lh\cos(\delta) - \frac{2}{\sqrt{3}}lb\sin(\delta)\sin(\alpha)}, \tag{10}$$

respectively.

The prestressability problem (conditions (6)) for these configurations was solved by Sultan et al. (2001) yielding:

$$q_{\mathrm{e}} = \left[\delta \quad \alpha \quad \delta \quad \alpha + \frac{4\pi}{3} \quad \delta \quad \alpha + \frac{2\pi}{3} \quad \delta \quad \alpha + \frac{2\pi}{3} \quad \delta \quad \alpha \quad \delta \quad \alpha + \frac{4\pi}{3} \quad \frac{5\pi}{3} \quad 0 \quad 0 \quad 0 \quad 0 \quad 2l\cos(\delta) - h\right]^{\mathrm{T}}, \tag{11}$$

where

$$h=\begin{cases}\dfrac{\cos(\delta)}{2\sin(\delta)\cos\left(\alpha+\frac{\pi}{6}\right)}\left(-\dfrac{b}{\sqrt{3}}+p+\sqrt{\dfrac{b^2}{3}-3p^2}\right) & \text{if } \alpha\neq\dfrac{\pi}{3},\\ \dfrac{l\cos(\delta)}{2} & \text{if } \alpha=\dfrac{\pi}{3},\end{cases} \tag{12}$$

with $p=l\sin(\delta)\cos(\alpha+\pi/6)$. These solutions exist if and only if α and δ satisfy the following conditions:

$$\frac{\pi}{6}<\alpha<\frac{\pi}{2},\quad 0<\delta<\frac{\pi}{2},$$

$$l\sin(\delta)\left|\cos\left(\alpha+\frac{\pi}{6}\right)\right|<\frac{b}{2\sqrt{3}}\quad\text{and}\quad\sin\left(\alpha+\frac{\pi}{6}\right)<\frac{3l\sin(\delta)}{2b}. \tag{13}$$

Sultan et al. (2001) showed that at any of these *symmetrical prestressable configurations* the state of stress is uniquely determined up to an arbitrary multiplicative positive scalar, P, called the *pretension coefficient*.

In the (α,δ,h) space the set of these prestressable configurations is defined by

$$\widehat{U}=\{(\alpha,\delta,h)\text{ with }(\alpha,\delta)\text{ satisfying conditions (13) and }h\text{ given by Eq. (12)}\}, \tag{14}$$

and is represented by an equilibrium surface. In the state space this surface corresponds to the equilibrium manifold which will be used in our deployment strategy.

The necessary rest-lengths of the saddle, vertical, and diagonal tendons which guarantee a symmetrical prestressable configuration (characterized by α, δ) and a prescribed pretension (P) are given by:

$$S_0=\frac{k_S S}{T_{0_S}P+k_S},\quad V_0=\frac{k_V V}{T_{0_V}P+k_V},\quad D_0=\frac{k_D D}{T_{0_D}P+k_D}. \tag{15}$$

Formulas for T_{0_S}, T_{0_V}, T_{0_D} in terms of α and δ are given in Sultan et al. (2001).

Using the linearized models of tensegrity structures dynamics, Sultan et al. (2002b) ascertained that these symmetrical prestressable configurations are asymptotically stable.

In the following we shall assume that the controls are the tendons rest-lengths. The *equilibrium manifold control set* it is then characterized by Eqs. (15). This is the set in which the controls will be allowed to take values during deployment.

5.3. Tendon control deployment

The deployment task is to erect the structure from an almost flat configuration to the nominal one, corresponding to the operating conditions. We assume that both the undeployed and the deployed configurations are symmetrical prestressable configurations as defined before, characterized by (α_u, δ_u) and (α_d, δ_d) respectively. The deployment process has to be performed such that all tendons are maintained in tension and the bars do not touch each other. No external forces or torques act on the structure ($F=0$).

In this example tendon control will be used to conduct the deployment. This procedure requires modification of the active lengths of the tendons. This task can be accomplished by motors attached, for example, at the end of the bars (or, if the bars are hollow, inside them). These motors work in the following way. For example the motor pulls a tendon and rolls it over a small wheel in such a way that its active length is shortened: the part of the tendon which is rolled over the motor wheel no longer contributes to the tendon tension. Hence this control procedure works as if the rest-length of the tendon would be shortened. Similarly, when the motor changes its sense of rotation, a portion of the inactive tendon becomes active, carrying force; hence the rest-length of the tendon increases. We call this procedure of tendon control, *rest-length control*.

5.4. Time optimal control

In the following we shall analyze the time optimal deployment control problem.

Since in this scenario we assume that the controls are the tendons rest-lengths, l_0, we can write the mathematical problem to be solved as

$$\begin{aligned} &\min_{l_0(t)} \quad T_{\mathrm{d}} \\ &\text{s.t.} \quad \dot{x} = f(x, l_0(t)), \quad x(0) = [q_{e_{\mathrm{u}}}^{\mathrm{T}}\ 0^{\mathrm{T}}]^{\mathrm{T}}, \quad x(T_{\mathrm{d}}) = [q_{e_{\mathrm{d}}}^{\mathrm{T}}\ 0^{\mathrm{T}}]^{\mathrm{T}}, \\ &\qquad l_0(0) = l_{0_{\mathrm{u}}}, \quad l_0(T_{\mathrm{d}}) = l_{0_{\mathrm{d}}}, \quad g_i(x, l_0) < 0, \quad i = 1, \ldots, N_{\mathrm{c}}, \quad l_0(t) \in L_0. \end{aligned} \tag{16}$$

The subscripts u and d refer to the undeployed and deployed configurations, respectively, l_0 is the vector of tendons rest-lengths, T_{d} is the deployment time, and g_i, $i = 1, \ldots, N_{\mathrm{c}}$, account for all of the inequality constraints (e.g. the distances between bars should be greater than a minimum value, tendons must be in tension, the forces experienced by all the elements must be less than the maximum admissible values). The control region, L_0, is the set in which the controls lie (e.g. a parallelepiped in the control space, situated in the first quadrant).

Time optimal control problems have been extensively treated in the literature. In the case of inequality path constraints the control law is in the class of piecewise continuous functions (Bryson and Ho, 1985). The solution is provided by the maximum principle (Pontryagin et al., 1962) and it usually consists of discontinuous control laws. For large systems of differential equations, like those used to describe structure's dynamics, the resulting two point boundary value problem is difficult to solve.

The problem can be simplified if we consider motions close to the symmetrical prestressable configurations class presented before. These configurations have some important advantages for our purpose: closed form (analytical) solutions for the generalized coordinates are available (Eq. (11)) as well as for the corresponding rest-lengths (Eqs. (15)), analytical expressions to describe the state of stress of the structure are also given (see Sultan et al., 2001), the clearance condition is easily checked (the bars axes of symmetry intersect only for $\alpha = \pi/6$), and all tendons are in tension. In the state space, this class is represented by a manifold to which both the undeployed and deployed configurations belong. We shall conduct the deployment such that its state space path is close enough to the equilibrium manifold by requiring that the controls, l_0, take values only in the symmetrical prestressable configurations manifold control set.

5.5. Numerical solution

The application of the previously proposed deployment strategy leads to the following methodology:

- $\forall t \in [0, T_{\mathrm{d}}]$ the rest-lengths are given by Eqs. (15) with $\alpha = \alpha_{\mathrm{e}}(t)$, $\delta = \delta_{\mathrm{e}}(t)$. The control variables are now $\alpha_{\mathrm{e}}(t)$ and $\delta_{\mathrm{e}}(t)$ and they represent functions of time which will be determined later.
- The initial and final conditions for the controls correspond to undeployed and deployed configurations respectively: $\alpha_{\mathrm{e}}(0) = \alpha_{\mathrm{u}}$, $\delta_{\mathrm{e}}(0) = \delta_{\mathrm{u}}$, $\alpha_{\mathrm{e}}(T_{\mathrm{d}}) = \alpha_{\mathrm{d}}$, $\delta_{\mathrm{e}}(T_{\mathrm{d}}) = \delta_{\mathrm{d}}$.
- Let $x_{\mathrm{d}}(t) = [q(t)^{\mathrm{T}}\ \dot{q}(t)^{\mathrm{T}}]^{\mathrm{T}}$ denote the corresponding *deployment path* (the state space trajectory of the dynamical system of Eqs. (3) and (4), with the time variant rest-lengths as described before.

The detailed equations of motion for two stage SVD tensegrity structures can be found in Sultan (1999).

- Let $x_{\mathrm{e}}(t) = [q_{\mathrm{e}}(t)^{\mathrm{T}}\ 0^{\mathrm{T}}]^{\mathrm{T}}$ denote the *equilibrium path* corresponding to $\alpha_{\mathrm{e}}(t)$, $\delta_{\mathrm{e}}(t)$ ($q_{\mathrm{e}}(t)$ is given by Eq. (11) with $\alpha = \alpha_{\mathrm{e}}(t)$, $\delta = \delta_e(t)$). In the (α, δ, h) space the equilibrium path represents a curve on the equilibrium surface, connecting the undeployed and deployed configurations.

- The control law, $(\alpha_e(t), \delta_e(t))$, has to be designed such that $\forall t \in [0, T_d]$, $\|q(t) - q_e(t)\| < \varepsilon_q$, $\|\dot{q}(t)\| < \varepsilon_{\dot{q}}$. Hence the deployment path can be made arbitrarily close to the equilibrium path by choosing the tolerances ε_q and $\varepsilon_{\dot{q}}$ small enough.

It is apparent that the closer the deployment path is to the equilibrium path (thus the smaller ε_q and $\varepsilon_{\dot{q}}$ are) the longer the deployment process is. Thus, minimizing the deployment time appears as a natural objective.

For simplicity we further assume that, for $t \in [0, T_d]$, $\alpha_e(t)$ and $\delta_e(t)$ are polynomials of a certain degree. This way the problem is transformed into a parameter optimization problem with inequality constraints, the parameters to be solved for being the polynomials coefficients.

We also relax the terminal condition $(x(T_d) = [q_{e_d}^T \ 0^T]^T)$ on the account that, being asymptotically stable, the deployed configuration will attract all neighboring solutions. Thus it is sufficient to get $x(T_d)$ close enough to $[q_{e_d}^T \ 0^T]^T$ and fix the control variables values to those corresponding to the deployed configuration: $\alpha_e(t \geqslant T_d) = \alpha_d$, $\delta_e(t \geqslant T_d) = \delta_d$.

After a change of coordinates to normalize time, $t = \tau T_d$, $\tau \in [0, 1]$, the mathematical statement of the minimum time deployment problem becomes:

$$\begin{aligned} &\min_{T_d, p_\alpha, p_\delta} \quad T_d \\ &\text{s.t.} \qquad T_d > 0 \text{ and } \forall \tau \in [0,1] : \|q(\tau) - q_e(\tau)\| < \varepsilon_q, \quad \|\dot{q}(\tau)\| < \varepsilon_{\dot{q}}, \quad (\alpha_e(\tau), \delta_e(\tau)) \in U, \end{aligned} \tag{17}$$

where

$$\delta_e(\tau) = p_\delta^T \tau_s, \quad \alpha_e(\tau) = p_\alpha^T \tau_s, \quad \tau_s = [1 \tau \cdots \tau^s]^T,$$

$$\delta_e(0) = \delta_u, \quad \delta_e(1) = \delta_d, \quad \alpha_e(0) = \alpha_u, \quad \alpha_e(1) = \alpha_d.$$

Here U is defined by conditions (13), p_α and p_δ are vectors of $\alpha_e(t)$ and $\delta_e(t)$ polynomials coefficients, whereas s is the degree of these polynomials, and $x(\tau) = [q(\tau)^T \ \dot{q}^T(\tau)]^T$ is the solution of:

$$\frac{dx}{d\tau} = f(x, l_0(\alpha_e(\tau), \delta_e(\tau)))T_d \quad \text{with the initial conditions } x_0 = [q_{e_u}^T \ 0^T]^T. \tag{18}$$

Thus a parameter constrained minimization problem has to be solved. The constraints, which have to be met $\forall \tau \in [0, 1]$, will be imposed only at the nodes of a *solution* grid of $[0, 1]$ and the corresponding solution checked on a finer one (the *test* grid). The parameter constrained minimization problem which results can be formally written as:

$$\begin{aligned} &\min_{T_d, p_\alpha, p_\delta} \quad T_d \\ &\text{s.t.} \qquad T_d > 0 \text{ and } g_i(T_d, p_\alpha, p_\delta) < 0, \ \ i = 1, \ldots, N_g, \end{aligned} \tag{19}$$

where $g_i(T_d, p_\alpha, p_\delta) < 0$, $i = 1, \ldots, N_g$, account for the inequality constraints imposed at the solution grid points.

This problem has been numerically solved using an exact penalty function combined with the Nedler–Meade method for optimization (see Sultan, 1999, for details).

5.6. Results

We shall next present some results obtained using the above procedure. We assume that the deployment takes place at a fixed pretension. For this fixed pretension, P, the bars are designed for buckling as shown by Sultan (1999) yielding:

$$m_{\mathrm{b}} = \rho \pi l \left(R^2 - \sqrt{R^4 - \frac{4 l^2 \gamma_{\mathrm{b}} C_0^{\mathrm{d}} P}{\pi^3 E_{\mathrm{b}}}} \right). \tag{20}$$

Here m_{b} is the mass of the bar designed to withstand buckling, γ_{b} is a safety coefficient, ρ is bar's density, E_{b} its Young's modulus, R the exterior radius of the bar (assumed to be a pipe), $C_0^{\mathrm{d}} P$ is the compressive force used for design.

Tendons are designed for maximum stress:

$$k_* = \frac{E_* T_{0_*}^{\mathrm{d}} P \gamma_{\mathrm{t}}}{\sigma_{*_{\max}}} \tag{21}$$

where $\sigma_{*_{\max}}$ is the maximum stress allowed in tendon * (* stands for S, V, D) and γ_{t} is a safety coefficient.

Because during deployment the structure takes configurations which are close to the equilibrium manifold we choose the design forces, $C_0^{\mathrm{d}} P$ and $T_{0_*}^{\mathrm{d}} P$, respectively, as the maximum values of the compression forces in bars and tensions in tendons over the set of all symmetrical prestressable configurations. Since P is assumed constant during deployment, we have

$$C_0^{\mathrm{d}} = \max_{(\alpha,\delta)\in U} (C_0), \quad T_{0_*}^{\mathrm{d}} = \max_{(\alpha,\delta)\in U} (T_{0_*}), \tag{22}$$

where U is defined by conditions (13) and formulas for C_0 and T_{0_*} in terms of α and δ can be found in Sultan et al. (2001). Choosing high values for the safety coefficients γ_{b} and γ_{t} we can account for the additional dynamical loads which occur.

The following geometric and material properties of the structure were considered:

$$\begin{aligned} &l = 0.4 \text{ m}, \quad b = 0.27 \text{ m}, \quad R = 0.01 \text{ m}, \quad E_{\mathrm{b}} = 7 \times 10^{10} \text{ N/m}^2, \quad \rho = 2800 \text{ kg/m}^3, \\ &E_* = 14 \times 10^{10} \text{ N/m}^2, \quad \sigma_{*_{\max}} = 2.5 \times 10^9 \text{ N/m}^2. \end{aligned} \tag{23}$$

Using the results of Sultan et al. (2001) we determined:

$$C_0^{\mathrm{d}} = 0.67, \quad T_{0_{\mathrm{S}}}^{\mathrm{d}} = T_{0_{\mathrm{D}}}^{\mathrm{d}} = 0.36, \quad T_{0_{\mathrm{V}}}^{\mathrm{d}} = 0.34. \tag{24}$$

The safety coefficients were considered $\gamma_{\mathrm{b}} = \gamma_{\mathrm{t}} = 4$.

The inertial properties of the structure (including the additional devices attached to bars such as electric motors to control deployment) and damping coefficients were considered

$$\begin{aligned} &m = m_{\mathrm{b}} + 0.4 \text{ kg}, \quad J = \frac{m l^2}{12} + 0.6 \text{ kg m}^2, \quad M_{\mathrm{t}} = 1 \text{ kg}, \quad J_1 = 3 \text{ kg m}^2, \quad J_2 = 4 \text{ kg m}^2, \\ &J_3 = 5 \text{ kg m}^2, \quad d = -0.9, \end{aligned} \tag{25}$$

where J_1, J_2, J_3 are the moments of inertia of the top with respect to $\hat{t}_1, \hat{t}_2, \hat{t}_3$ respectively, M_{t} is the mass of the top and J is the transversal moment of inertia of a bar.

We present in Table 1 the minimum deployment time obtained for linear ($s = 1$) and quadratic ($s = 2$) control laws, $\alpha_{\mathrm{e}}(t)$ and $\delta_{\mathrm{e}}(t)$. The tolerances were chosen $\varepsilon_q = 0.1$, $\varepsilon_{\dot{q}} = 0.2$, the solution grid was uniform with 30 points and the testing grid was twice as dense. The deployed and undeployed configurations were

Table 1
Minimum deployment time (s)

s/P	100	200	300	400	500
1	13.33	14.02	13.14	12.63	13.15
2	12.64	14.02	13.14	12.47	11.75

$\alpha_u = 69$, $\delta_u = 85$, $\alpha_d = 50$, $\delta_d = 55$ (all in degrees). The corresponding height of the structure was 0.04 m and 0.41 m respectively.

The quadratic laws are more performant than the linear ones (except for $P = 200$ and $P = 300$ when the coefficients of the quadratic terms in $\alpha_e(t)$ and $\delta_e(t)$ were practically negligible). This is no surprise, since the quadratic polynomials set contains the linear ones. It is expected that the performance increases with the degree of the polynomials, s. However, it is desired to implement as simple as possible controls, e.g. low degree polynomials.

We can compute the energy required to perform the deployment if we apply the energy transformation law:

$$W = U_d - U_u + K_1 - T_d \sum_{i=1}^{6} \int_0^1 M_i^T \omega_i^r \, d\tau, \tag{26}$$

Table 2
Control energy (J)

s/P	100	200	300	400	500
1	0.1557	0.1398	0.1358	0.1374	0.1201
2	0.1089	0.0865	0.0852	0.0827	0.0810

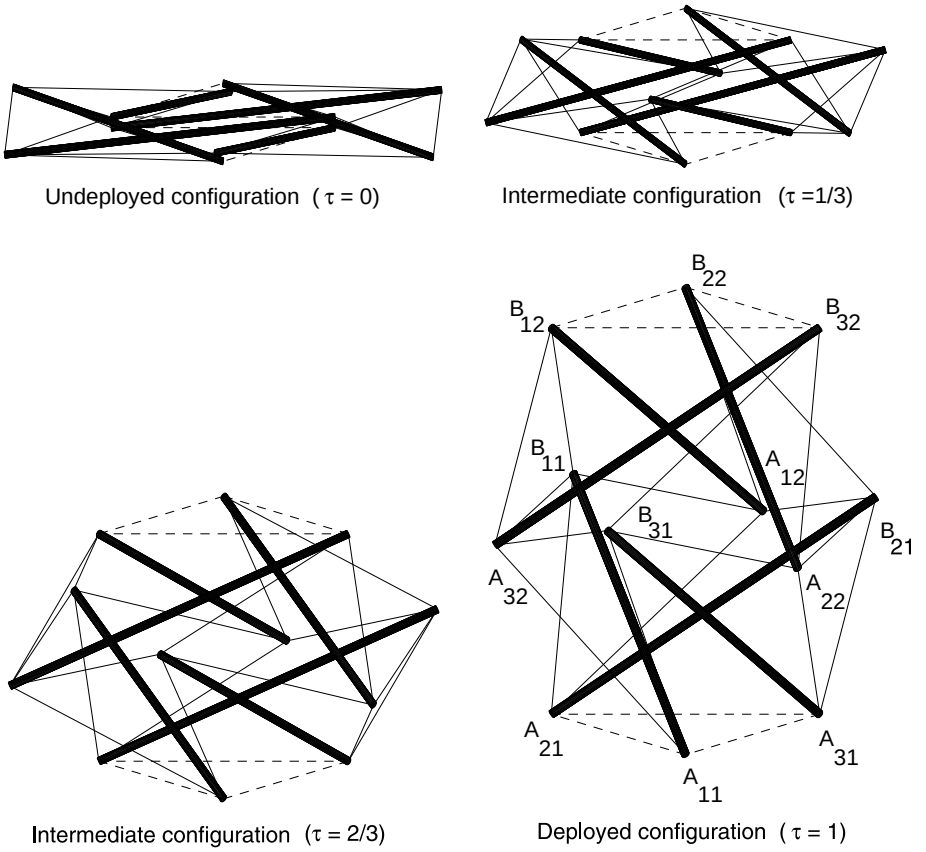

Fig. 3. Deployment sequence for $P = 300$, quadratic polynomials.

where U_* represents the elastic potential energy at the * configuration, K_1 is the kinetic energy when deployment is completed (at $\tau = 1$) and $T_d \sum_{i=1}^{6} \int_0^1 M_i^T \omega_i^r \, d\tau$ is the work of the friction torques. The results are given in Table 2.

The energy required for deployment decreases with increasing pretension and polynomials degree (s). It is important to note that, if $W < 0$, it means that energy is generated through the deployment process: the potential energy at the undeployed configuration is converted in kinetic and potential energy, work against the friction forces and reusable energy.

Fig. 3 gives the deployment sequence corresponding to $P = 300$ and quadratic polynomials. The Euclidean norms of the nondimensional errors variations ($\hat{q} - \hat{q}_e$ and $\dot{\hat{q}}$ vs τ) are shown in Figs. 4 and 5 (the nondimensional generalized coordinates are obtained by dividing lengths—X, Y, Z—through l and angles through 1 rad). Fig. 4 reveals that the deployment path is practically identical with the equilibrium path. The difference is the nonzero velocity (see Fig. 5) which finally results in deployment. Fig. 6 shows how the

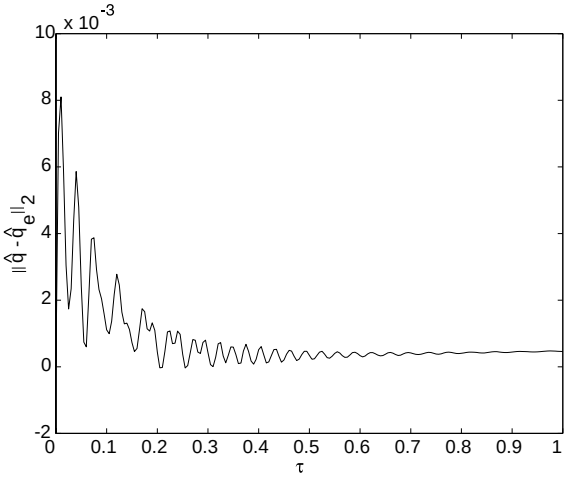

Fig. 4. Error between the deployment and equilibrium path.

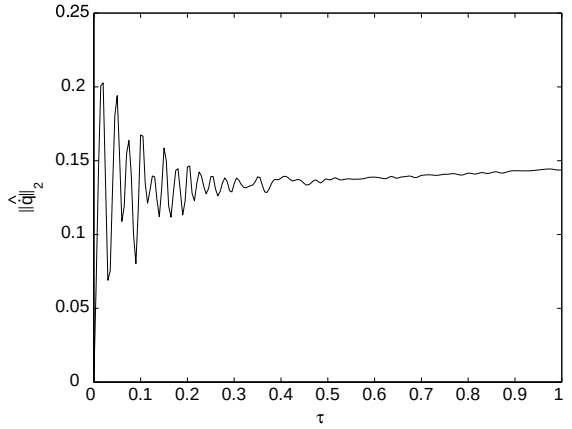

Fig. 5. Nondimensional generalized velocities norm for the deployment path.

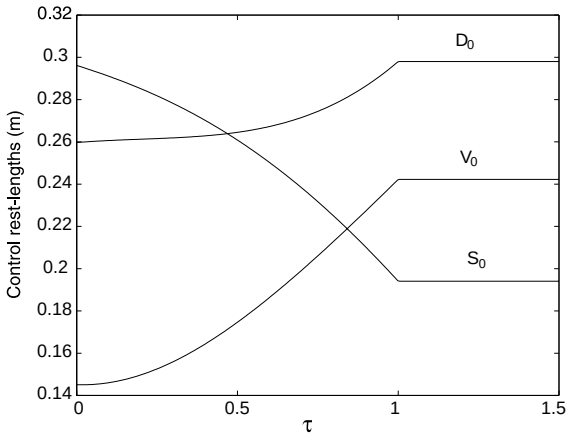

Fig. 6. Rest-length variations during deployment.

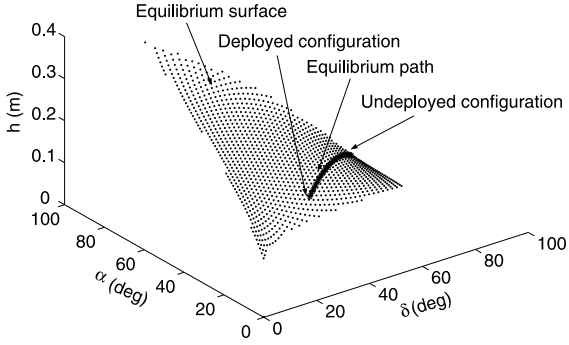

Fig. 7. Equilibrium path and equilibrium surface.

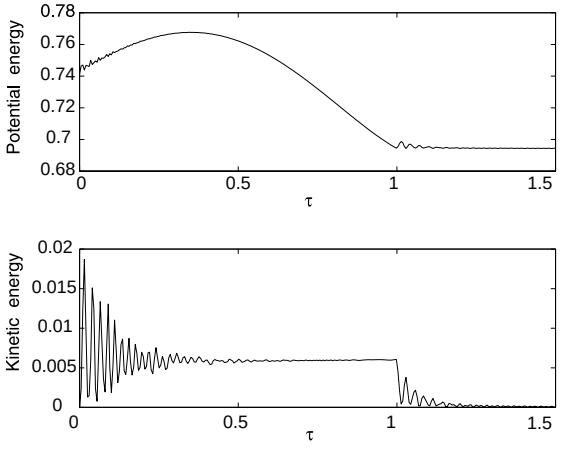

Fig. 8. Potential and kinetic energies variations during deployment.

rest-lengths of the saddle (S_0), vertical (V_0), and diagonal (D_0) tendons vary during deployment; after the process is completed (for $\tau > 1$) they are fixed to the deployed configuration values. Fig. 7 shows the equilibrium path. Finally, Fig. 8 gives the variations in potential and kinetic energies. We ascertain that after the controls are fixed at the deployed configuration values the kinetic energy rapidly decays, indicating stabilization at the deployed configuration.

The rapid oscillations in the initial and final stages of the deployment are due to the fact that the time derivatives of the controls are not continuous at $\tau = 0$ and $\tau = 1$, hence the high frequency modes of the structure are excited. This problem can easily be fixed by using more smooth controls as shown in the next example.

6. Tensegrity tower deployment

In the following we present another application of the proposed deployment strategy to a tensegrity tower. Sultan (1999) analyzed tensegrity towers with three to ten stages and discovered equilibrium manifolds which can be used for deployment.

6.1. Tensegrity tower description

The tensegrity tower analyzed in this article is composed of three stages, each stage having three bars (Fig. 1). The end points of a bar are labeled A_{ij} and B_{ij}, $i = 1, 2, 3$, $j = 1, 2, 3$. Stage number j is composed of bars $A_{ij}B_{ij}$, $i = 1, 2, 3$. The bars of the first stage are attached via ball and socket joints to a base, and the bars of the third stage are attached via ball and socket joints to a top. The end points of the bars are connected through a total of 33 tendons.

For mathematical modeling the same assumptions as for the two stage SVD structure analyzed before have been made (see Sultan, 1999, for details). Two reference frames are introduced: the inertial and the top reference frames, $\hat{b}_1$, $\hat{b}_2$, $\hat{b}_3$, and $\hat{t}_1$, $\hat{t}_2$, $\hat{t}_3$ respectively, defined as in the two stage SVD case. For simplicity we assume that $\hat{t}_1$, $\hat{t}_2$, $\hat{t}_3$ is a central principal reference frame for the top.

The *independent generalized coordinates* which describe the configuration of this system are:

- δ_{ij}, α_{ij}, the declination and the azimuth of bar $A_{ij}B_{ij}$, defined as in the two stage SVD case.
- x_{i2}, y_{i2}, z_{i2}, the inertial Cartesian coordinates of the mass center of bar $A_{i2}B_{i2}$.
- ψ, ϕ, θ, the Euler angles for a 3-1-2 sequence to characterize the orientation of the top reference frame with respect to the inertial frame.
- X, Y, Z, the inertial Cartesian coordinates of the geometric center of $B_{13}B_{23}B_{33}$.

6.2. Equilibrium manifold

Sultan (1999) discovered an equilibrium manifold consisting of *symmetrical cylindrical prestressable configurations*. These configurations are characterized as follows. Triangles $A_{11}A_{21}A_{31}$ and $B_{13}B_{23}B_{33}$ are congruent, equilateral triangles of side length b, all bars have equal length, l, and the same declination, δ. Bars $A_{11}B_{11}$, $A_{22}B_{22}$, $A_{33}B_{33}$, are parallel, bars $A_{21}B_{21}$, $A_{32}B_{32}$, $A_{13}B_{13}$ are parallel, bars $A_{31}B_{31}$, $A_{12}B_{12}$, $A_{23}B_{23}$ are parallel, all nodal points A_{ij}, B_{ij}, $i = 1, 2, 3$, $j = 1, 2, 3$, lie on the surface of a rectangular cylinder, the projections onto the base of the jth saddle points, A_{3j+1}, B_{1j}, B_{3j}, A_{2j+1}, B_{2j}, A_{1j+1}, make a regular hexagon, planes $A_{1j}A_{2j}A_{3j}$ and $A_{1j+1}A_{2j+1}A_{3j+1}$, $j = 1, 2$, are parallel, the distance between $A_{1j+1}A_{2j+1}A_{3j+1}$ and $B_{1j}B_{2j}B_{3j}$ is the same for all $j = 1, 2$, and it is called the overlap, h. The overlap is positive if $B_{1j}B_{2j}B_{3j}$ is closer to $A_{11}A_{21}A_{31}$ than $A_{1j+1}A_{2j+1}A_{3j+1}$.

At a symmetrical cylindrical prestressable configuration there are six different tendons tensions. The tendons which have the same tension are grouped as follows: group D_1: $A_{11}A_{12}$, $A_{21}A_{22}$, $A_{31}A_{32}$, $B_{12}B_{13}$, $B_{22}B_{23}$, $B_{32}B_{33}$, group V_1: $A_{11}B_{21}$, $A_{21}B_{31}$, $A_{31}B_{11}$, $A_{33}B_{13}$, $A_{13}B_{23}$, $A_{23}B_{33}$, group S_1: $B_{11}A_{12}$, $B_{21}A_{22}$, $B_{31}A_{32}$, $B_{12}A_{13}$, $B_{22}A_{23}$, $B_{32}A_{33}$, group S_1': $B_{21}A_{12}$, $B_{31}A_{22}$, $B_{11}A_{32}$, $B_{22}A_{13}$, $B_{32}A_{23}$, $B_{12}A_{33}$, group V_2: $A_{12}B_{32}$, $A_{22}B_{12}$, $A_{32}B_{22}$, group D_2: $A_{12}A_{33}$, $A_{22}A_{13}$, $A_{32}A_{23}$, $B_{11}B_{32}$, $B_{21}B_{12}$, $B_{31}B_{22}$. For simplicity, in the following we assume that the tendons in each group are identical, their rest-lengths being labeled as follows: group D_1, D_{10}, group V_1, V_{10}, group S_1, S_{10}, group S_1', S_{10}', group V_2, V_{20}, group D_2, D_{20}.

The equilibrium manifold consisting of symmetrical cylindrical prestressable configurations has been computed as shown in Sultan (1999). In the (α, h) space it is represented by a curve segment whose end points are characterized by the fact that the tensions in some of the tendons become zero. The corresponding values of the independent generalized coordinates are:

$$\delta_{ij} = \delta, \quad \text{where } i = 1,2,3, \ \ j = 1,2,3,$$

$$z_{i2} = \frac{3}{2} l \cos(\delta) - h, \quad \text{where } i = 1,2,3,$$

$$\alpha_{11} = \alpha_{22} = \alpha_{33} = \alpha, \quad \alpha_{21} = \alpha_{32} = \alpha_{13} = \alpha + \frac{4\pi}{3}, \quad \alpha_{31} = \alpha_{12} = \alpha_{23} = \alpha + \frac{2\pi}{3},$$

$$\begin{aligned} x_{12} &= -\frac{b}{2} - \frac{l}{2}\sin(\delta)\cos(\alpha_{12}), \quad y_{12} = \frac{\sqrt{3}}{6} b - \frac{l}{2}\sin(\delta)\sin(\alpha_{12}), \\ x_{22} &= \frac{b}{2} - \frac{l}{2}\sin(\delta)\cos(\alpha_{22}), \quad y_{22} = \frac{\sqrt{3}}{6} b - \frac{l}{2}\sin(\delta)\sin(\alpha_{22}), \\ x_{32} &= -\frac{l}{2}\sin(\delta)\cos(\alpha_{32}), \quad y_{32} = -\frac{\sqrt{3}}{3} b - \frac{l}{2}\sin(\delta)\sin(\alpha_{32}), \end{aligned}$$

$$\phi = \theta = X = Y = 0, \quad Z = 3l\cos(\delta) - 2h, \quad \psi = 2\alpha. \tag{27}$$

Here α is the azimuth of bar $A_{11}B_{11}$ and is related to δ by the constraint that all nodal points lie on the surface of a cylinder:

$$\sin(\delta) = \frac{2b\sin\left(\alpha + \frac{\pi}{3}\right)}{\sqrt{3}l}. \tag{28}$$

The overlap h is obtained by solving a cubic equation in h (see Sultan, 1999, for details).

At a symmetrical cylindrical prestressable configuration there is sufficient clearance between bars and the tensions are, as in the two stage SVD tensegrity structure case, uniquely determined up to a positive multiplicative scalar, the pretension coefficient, $P : T(q) = PT_0$ (see Sultan and Skelton, in press, for details). It has also been numerically ascertained that all these configurations are asymptotically stable (see Sultan, 1999).

The rest-lengths, l_{0_j}, which guarantee such a prestressable configuration and a certain pretension, P, can be computed as

$$l_{0_j} = \frac{k_j l_j}{T_{0_j} P + k_j}, \quad j = 1, \ldots, 33. \tag{29}$$

where k_j is the stiffness and l_j represents the length of tendon j evaluated at a symmetrical cylindrical prestressable configuration (see Sultan and Skelton, in press, for formulas of l_j, T_{0_j} in terms of α). These

formulas characterize the symmetrical cylindrical prestressable configurations manifold control set and they will be used for deployment.

7. Prescribed time deployment

The deployment problem consists in changing the configuration of the tensegrity tower from a symmetrical cylindrical prestressable configuration to another symmetrical cylindrical prestressable configuration.

The previously developed deployment strategy will be applied assuming that the deployment time, T_d, is prescribed and that rest-length control is used. During deployment the rest-lengths take values in the symmetrical cylindrical prestressable configurations manifold control set, hence they are given by Eqs. (29) with α replaced by $\alpha_e(t)$. Here $\alpha_e(t)$ is a function of time determined such that it respects the following conditions: it is of class C^1 on $\mathbb{R}$, its end points values correspond to the undeployed and deployed configurations respectively ($\alpha_e(0) = \alpha_u, \alpha_e(T_d) = \alpha_d$), and it is a polynomial of the lowest possible degree. These conditions lead to:

$$\alpha_e(t) = \alpha_u + \frac{30}{T_d^5}(\alpha_d - \alpha_u)\left(\frac{t^5}{30} - \frac{t^4}{6}(t - T_d) + \frac{t^3}{3}(t - T_d)^2\right). \tag{30}$$

The function $\delta_e(t)$ is given by the cylindrical constraint:

$$\delta_e(t) = \arcsin\left(\frac{2b}{\sqrt{3}l}\left(\sin\left(\alpha_e(t) + \frac{\pi}{3}\right)\right)\right). \tag{31}$$

These formulas guarantee smooth transitory regimes because the controls are of class C^1 on $\mathbb{R}$ (first order time derivatives are continuous).

In this example we do not seek the optimization of any performance index hence the numerical solution is very simple. The nonlinear equations of motion of the tensegrity tower (see Sultan, 1999, for details) are numerically integrated using the time variant controls given by Eq. (29) in which α is replaced by $\alpha_e(t)$ as discussed before, and with the initial conditions given by the undeployed symmetrical cylindrical prestressable configuration. The resulting numerical solution, the *deployment path*, is used to check (on a dense grid) if certain conditions are met during deployment (e.g. the tendons are always in tension, the bars do not touch, etc.). If any of these conditions is violated, then the deployment time, T_d, should be increased.

The equilibrium path, defined as the state space curve parameterized by $\alpha_e(t)$, is, in this case, represented by a segment of the equilibrium curve in the (α, h) space.

7.1. Numerical results

As in the two stage SVD case the tendons can be designed to an upper bound on the maximum tension on the equilibrium manifold under consideration and the bars to an upper bound on the buckling force on the same manifold (see Sultan and Skelton, in press, for formulas of these forces).

For the numerical example presented next, the following characteristics have been considered:

$$\begin{aligned} &l = 0.4 \text{ m}, \quad b = 0.27 \text{ m}, \quad k_j = 1000 \text{ N}, \quad j = 1, \ldots, 33, \quad P = 500, \ d = -3, \quad M_t = 1 \text{ kg}, \\ &J_1 = 3 \text{ kg m}^2, \quad J_2 = 4 \text{ kg m}^2, \quad J_3 = 5 \text{ kg m}^2, \quad J = 1 \text{ kg m}^2, \quad m = 0.4 \text{ kg}. \end{aligned} \tag{32}$$

The initial and final configurations were

$$\alpha_u = -23^\circ, \quad \alpha_d = 5^\circ. \tag{33}$$

The corresponding height of the structure was 0.42 and 0.67 m respectively. The deployment time has been enforced to be $T_d = 20$ s.

Our numerical simulations indicated that the error between the deployment path and the equilibrium path is, as in the two stage SVD tensegrity structure case, very small. The tendons are always in tension during deployment and the clearance between bars is sufficient.

Fig. 9 shows a sequence of configurations during deployment. The time histories of the controls (the six tendons rest-lengths S_{10}, S'_{10}, V_{10}, V_{20}, D_{10}, D_{20}) are given in Fig. 10. Fig. 11 shows the time history of the height of the structure indicating that, due to the use of C^1 controls, the variation is smooth and the structure attains the desired configuration in *exactly* the prescribed deployment time, T_d.

A performance index can be introduced, as in the two stage SVD case, and an optimal problem can be solved (e.g. we can determine the deployment time such that the deployment and equilibrium paths are close enough, or such that the energy is minimized, etc.). Other generalizations might allow for the variation of P and optimization over it (e.g. P can be allowed to vary during deployment).

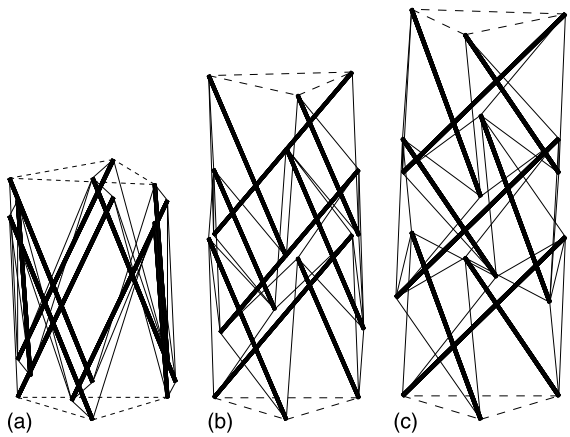

Fig. 9. Deployment sequence of the tower, from left to right: initial, intermediate, and final configuration.

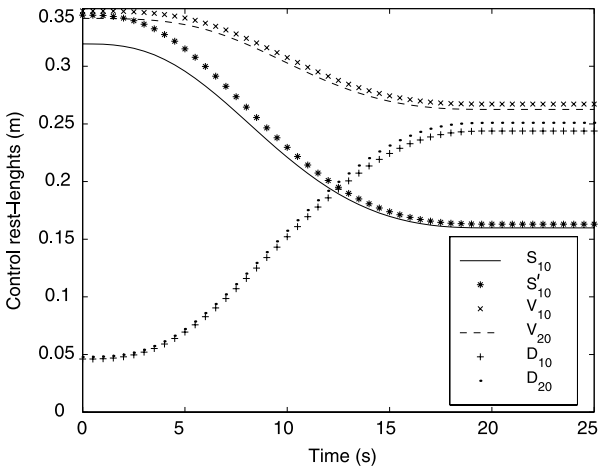

Fig. 10. Controls variation during deployment of the three stage tower.

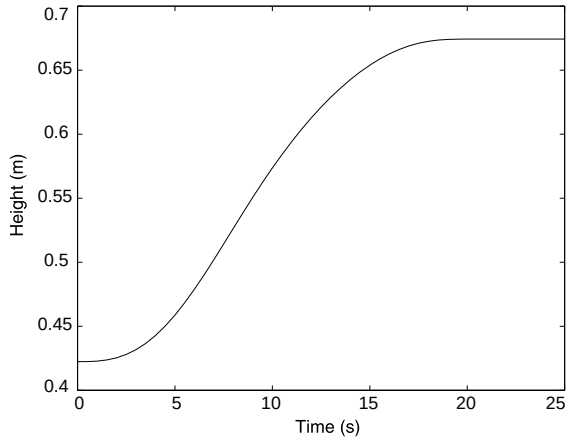

Fig. 11. Height time history of the three stage tower deployment.

8. Conclusions

A continuous time deployment control strategy for tensegrity structures is proposed, based on the existence of an equilibrium manifold. Deployment can be conducted such that the state space deployment trajectory is close enough to the equilibrium manifold and the structure smoothly evolves from one configuration to another.

Two examples are given, one showing a time optimal deployment of a relatively simple structure, the other the prescribed deployment time of a more complex structure. Our results indicate that the strategy can be successfully applied, yielding very reasonable deployment times (around 12 s) to erect the first structure from a height of 0.04–0.41 m. The second example shows that using more smooth controls, the structure can be deployed without exciting its high frequency modes of oscillations in a prescribed, finite time.

One apparent deficiency of this procedure is that it assumes that all tendons are controlled (as opposed to other procedures in which fewer elements are controlled). However this can be seen as an advantage because it allows the structure to assume many other shapes (e.g. it can turn into an arbitrary shape). Our procedure can be easily generalized to deployment or reconfiguration between very different shapes. The apparent deficiency of having to control too many tendons can be overcome by connecting several tendons together and using only one motor to control them.

The procedure presented herein can also be used for deployment of other structures (not only tensegrity). It can actually be used as a method of controlling nonlinear systems between their equilibrium states using equilibrium manifolds.

References

Bryson, A.E., Ho, Y.C., 1985. Applied Optimal Control. Hemisphere, Washington.

Calladine, C.R., 1978. Buckminster Fuller's tensegrity structures and Clerk Maxwell's rules for the construction of stiff frames. Int. J. Solids Struct. 14, 161–172.

Connelly, R., Whiteley, W., 1996. Second-order rigidity and prestress stability for tensegrity frameworks. SIAM J. Discrete Math. 9 (3), 453–491.

Djouadi, S., Motro, R., Pons, J.C., Crosnier, B., 1998. Active control of tensegrity systems. ASCE J. Aerospace Eng. 11 (2), 37–44.

Fuller, R.B., 1975. Synergetics, Explorations in the Geometry of Thinking. Collier Macmillan Publishers, London.

Furuya, H., 1992. Concept of deployable tensegrity structures in space application. Int. J. Space Struct. 7 (2), 143–151.

Hanaor, A., 1988. Prestressed pin-jointed structures—flexibility analysis and prestress design. Comput. Struct. 28 (6), 757–769.

Hanaor, A., 1992. Aspects of design of double layer tensegrity domes. Int. J. Space Struct. 7 (2), 101–113.
Kanchanasaratool, N., Williamson, D., 2002. Modeling and control of class NSP tensegrity structures. Int. J. Control 75 (2), 123–139.
Kebiche, K., Kazi-Aoual, M.N., Motro, R., 1999. Geometrical non-linear analysis of tensegrity systems. Eng. Struct. 21 (9), 864–876.
Motro, R., Najari, S., Jouanna, P., 1986. Static and dynamic analysis of tensegrity systems. In: Proceedings of the ASCE International Symposium on Shell and Spatial Structures: Computational Aspects. Springer Verlag, New York, pp. 270–279.
Motro, R., 1996. Structural morphology of tensegrity systems. Int. J. Space Struct. 11 (1 and 2), 25–32.
Murakami, H., 2001. Static and dynamic analyses of tensegrity structures. Part 1: nonlinear equations of motion. Int. J. Solids Struct. 38, 3599–3613.
Murakami, H., Nishimura, Y., 2001a. Initial shape finding and modal analyses of cyclic right-cylindrical tensegrity modules. Comput. Struct. 79, 891–917.
Murakami, H., Nishimura, Y., 2001b. Static and dynamic characterization of regular truncated icosahedral and dodecahedral tensegrity modules. Int. J. Solids Struct. 38, 9359–9381.
Nishimura, Y., Murakami, H., 2001. Initial shape finding and modal analyses of cyclic frustum tensegrity modules. Comput. Methods Appl. Mech. Eng. 190, 5795–5818.
Oppenheim, I.J., Williams, W.O., 2001a. Vibration of an elastic tensegrity structure. Eur. J. Mech. A/Solids 20 (6), 1023–1031.
Oppenheim, I.J., Williams, W.O., 2001b. Vibration and damping in a 3 bar tensegrity structure. ASCE J. Aerospace Eng. 14 (3), 85–91.
Pellegrino, S., Calladine, C.R., 1986. Matrix analysis of statically and kinematically indetermined frameworks. Int. J. Solids Struct. 22 (4), 409–428.
Pontryagin, L.S., Boltyanskii, V.G., Gamkrelidze, R.V., Mishchenko, E.F., 1962. The Mathematical Theory of Optimal Processes. Interscience Publishers, New York.
Pugh, A., 1976. An Introduction to Tensegrity. University of California Press, Berkeley.
Skelton, R.E., Sultan, C., 1997. Controllable tensegrity, a new class of smart structures. In: Proceedings of the SPIE 4th Symposium on Smart Structures and Materials, vol. 3039, pp. 166–177.
Sultan, C., Skelton, R.E., 1997. Integrated design of controllable tensegrity structures. In: Proceedings of the ASME International Congress and Exposition, vol. 54, pp. 27–37.
Sultan, C., Skelton, R.E., 1998a. Force and torque smart tensegrity sensor. In: Proceedings of the SPIE 5th Symposium on Smart Structures and Materials, vol. 3323, pp. 357–368.
Sultan, C., Skelton, R.E., 1998b. Tendon control deployment of tensegrity structures. In: Proceedings of the SPIE 5th Symposium on Smart Structures and Materials, vol. 3323, pp. 455–466.
Sultan, C., Skelton, R.E., in press. Tensegrity structures prestressability investigation. Int. J. Space Struct.
Sultan, C., Corless, M., Skelton, R.E., 1999. Peak to peak control of an adaptive tensegrity space telescope. In: Proceedings of the SPIE 6th Symposium on Smart Structures and Materials, vol. 3667, pp. 190–201.
Sultan, C., Corless, M., Skelton, R.E., 2000. Tensegrity flight simulator. Journal Guid. Control Dynam. 23 (6), 1055–1064.
Sultan, C., Corless, M., Skelton, R.E., 2001. The prestressability problem of tensegrity structures: Some analytical solutions. Int. J. Solids Struct. 38–39, 5223–5252.
Sultan, C., Corless, M., Skelton, R.E., 2002a. Symmetrical reconfiguration of tensegrity structures. Int. J. Solids Struct. 39, 2215–2234.
Sultan, C., Corless, M., Skelton, R.E., 2002b. Linear dynamics of tensegrity structures. J. Eng. Struct. 24, 671–685.
Sultan, C., 1999. Modeling, design, and control of tensegrity structures with applications. Ph.D. dissertation, Purdue University, School of Aeronautics and Astronautics, 200 p.
Tibert, A.G., Pellegrino, S., 2002. Deployable tensegrity reflectors for small satellites. J. Spacecraft Rockets 39 (5), 701–709.
Vassart, N., Motro, R., 1999. Multiparametered formfinding method: application to tensegrity systems. Int. J. Space Struct. 14 (2), 147–154.
Wang, B.B., Liu, X.L., 1996. Integral tension research in double-layer tensegrity grids. Int. J. Space Struct. 11 (4), 349–362.